Electronic Supplementary Information

Charge Polarization at Catalytic Metal-Support Junctions

Part A: Kelvin Probe Force Microscopy Results of Noble Metal Nanoparticles

Tobias Kittel[1] and Emil Roduner[1,2]*

[1] Institute of Physical Chemistry, University of Stuttgart,

Pfaffenwaldring 55, D-70569 Stuttgart, Germany

[2] Department of Chemistry, University of Pretoria, Pretoria 0002, Republic of South Africa

Verification of the sign of the Kelvin potential

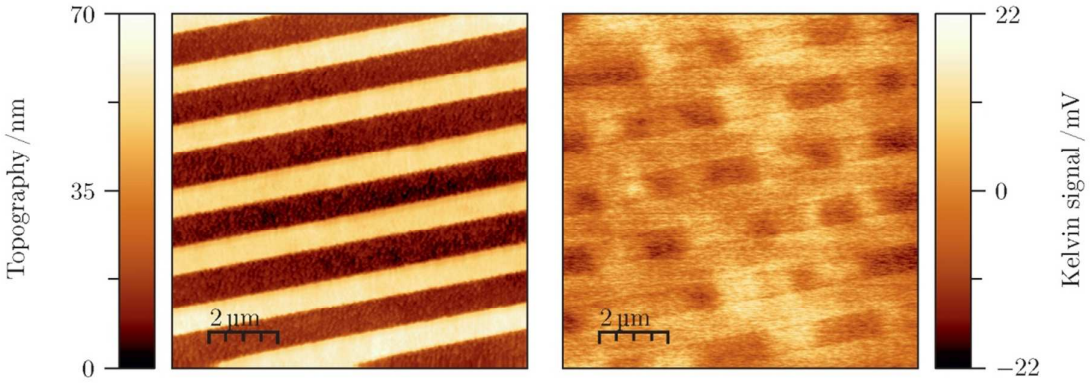

Figure S1: Topography of groove structure (left) and Kelvin signal (right) of a commercial CD-RW after removal of the protecting polymer layer. The bright, polycrystalline regimes on the rims between the grooves represent binary 1, the dark, amorphous regimes binary 2 with *ca.* 40 mV lower potential.

General energy level scheme of Schottky contacts

The situation of band gaps in a Schottky contact is shown in Figure S2. In metals, the energy level that is simultaneously the upper edge of the valence band VB and the lower edge of the conduction band CB is called the Fermi energy E_F. At finite temperature some of the electrons are excited thermally from the conduction band to the valence band. In semiconductors and in insulators the two edges are separated by the band gap energy E_G which amounts to up to several eV so that there is negligible excitation from the VB to the CB at ambient temperature. This can be changed by doping a semiconductor with an element which has more valence electrons (donor doping for n-type semiconductors) or less valence electrons (acceptor doping for p-type semiconductors) than the semiconductor, which leads to new states (defect states) slightly below the lower CB edge or somewhat above the VB edge, respectively. The Fermi energy around which excitation/depopulation occurs in thermal equilibrium is then between the new state and the closer band edge. In metal oxides, these defect states are often oxygen vacancies or substitutional HO^- states which leave an electron in the conduction band or attached to a metal cation, reducing it by one charge. The oxides are therefore seen as close analogs of n-type semiconductors.[1,2]

In a Schottky junction the metal is in contact with the semiconductor. For the metals used in this work, Pt, Pd and Rh, E_F lies within the band gap of the oxides TiO_2 and CeO_2 (Figure S3). In the absence of acceptor defect states no metal electrons are transferred onto the oxide support, but the presence of empty acceptor states in p-type semiconductors makes such a transfer possible. The transfer leads to charge polarization at the interface (right hand side of Figure S2). With occupied donor states in n-type semiconductors the electron transfer is from the semiconductor to the support, which leads to the opposite charge polarization. The relative position of the semiconductor band edges, of the defect states and of E_F of the metal are thus essential for a polarization to occur. This is seen in particular for the case of Pt on an Al_2O_3

support (lowest entry in Figure S3) where E_F of the metal lies above the lower CB band edge so that there is a large polarization already in the absence of defect states, and the introduction of defect states does not change this significantly.

In accord with earlier statements in literature (see main text) it is assumed here that adding or subtracting charge from the metal particle will change its (electro-)chemical potential and thus its ability to participate in catalytic redox or bond breaking/bond formation reactions. It is the purpose of this work to give specific evidence that such a charge polarization exists.

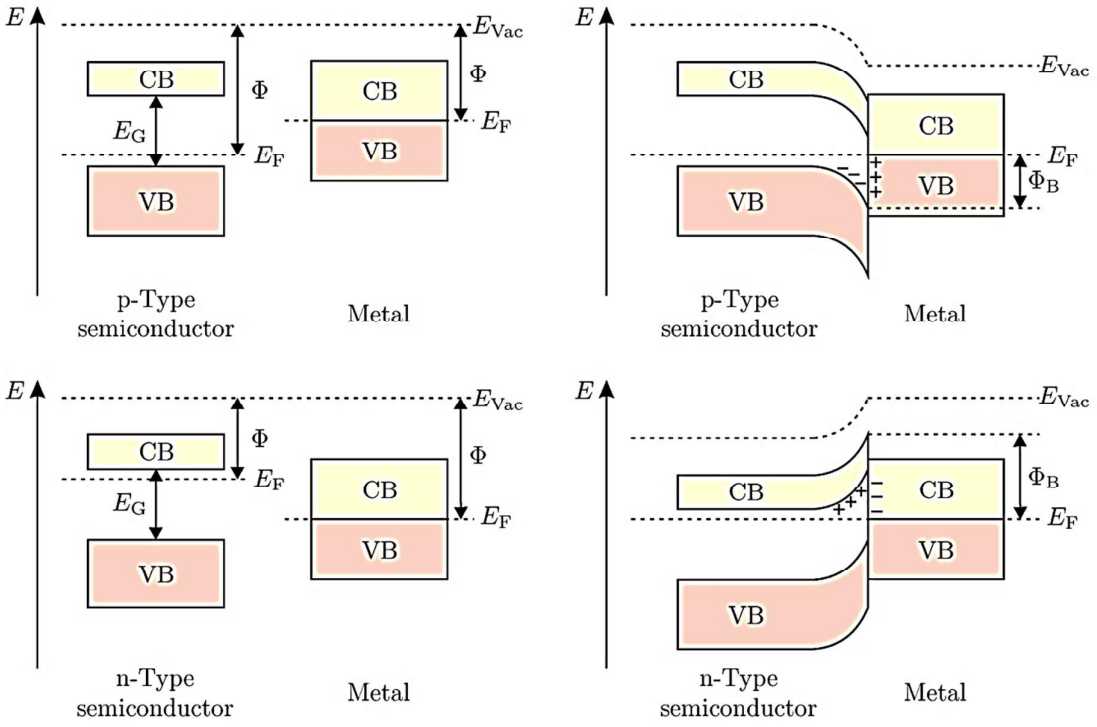

Figure S2: Energy level schemes of Schottky contacts between *p*-type (upper entries) and *n*-type (lower entries) semiconductors and a metal in the absence (left entries) and the presence (right entries) of thermal equilibrium. The position of the valence band (VB) and the conduction band (CB), the band gap (E_G) and the work functions Φ which is determined by the difference between the vacuum energy E_{Vac} and the Fermi levels E_F are indicated (Figure in analogy to Ref. 3).

Band level schemes of metal-semiconductor Schottky junctions in present work

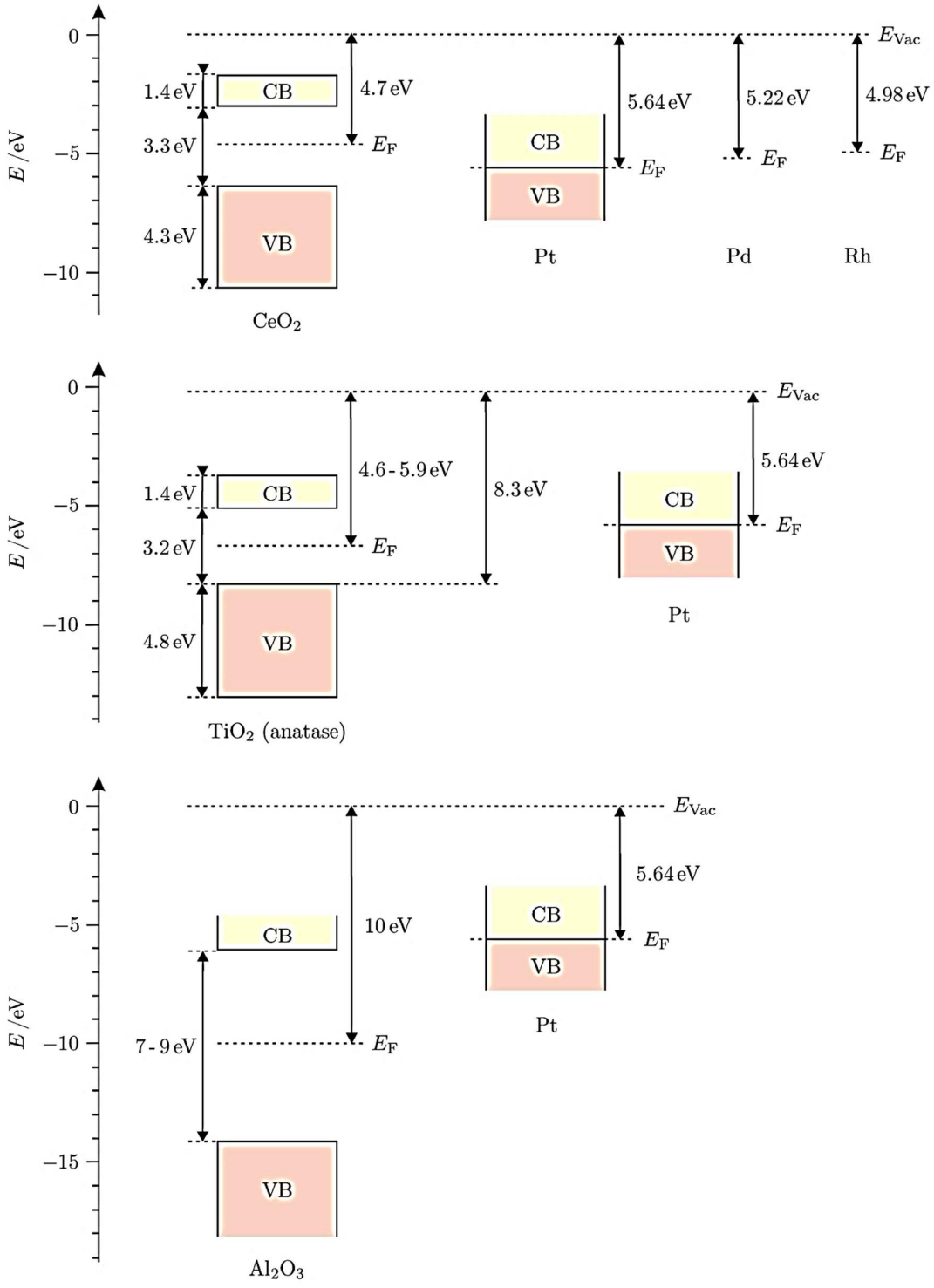

Figure S3: Specific energetic situation in present metal-semiconductor pairs, assuming the Fermi energy level in the band gap center (Figure prepared based on literature values). Values are based on Refs. 1, 4-13.

Effects of finite AFM tip radius

Atomic resolution can be obtained only when extremely sharp or functionalized AFM tips are used. However, electrically conductive tips require a coating, which leads to a tip radius R_{tip} of ~25 nm as specified by the provider. The finite tip size leads to a washing out of the true crystallite shape and of any structure of its facets, as illustrated in Figure S4a). Assuming a spherical tip shape and a given shape of the particle the broadening of the true particle size, R^* compared with the observed size R can be calculated for different values of the particle height H. The curves obtained are shown in Figure S4b)) and used for the particle size correction to obtain R^* from R (the present work assumes only paraboloid shape particles). Very small particles can appear up to six times larger than their true size, which demonstrates the necessity of corrections for the quantitative analysis. Measurements of each metal-support pair were performed with the same tip, but a fresh tip with a possibly slightly different radius was used for each new pair, which may result in limited comparability of the R^* values for different pairs.

The Kelvin probe measurements are less affected by the tip size effect since they are performed with a retracted tip that avoids contact with the particle. Nevertheless, there are some concerns about the approximation of a point-like tip on the Kelvin signal. These are discussed in a subchapter of the companion paper.

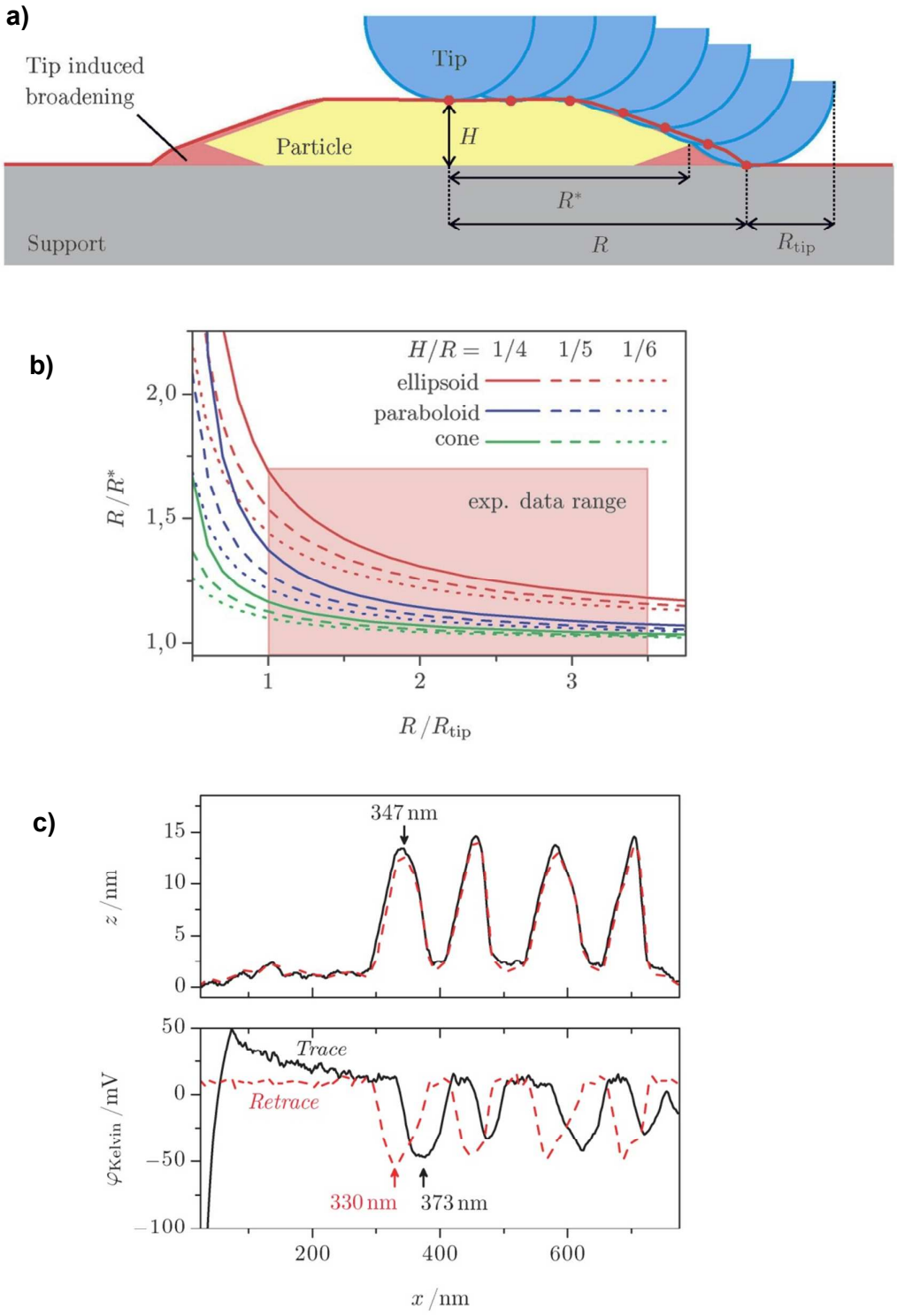

Figure S4: a) Schematic presentation of the broadening effect on the measured particle size due to finite AFM tip size R_{tip}. b) Enhancement of apparent particle radius R relative to its true value R^* as a function of R relative to the tip radius R_{tip}, given for three different relative

particle heights *H*/*R* and different particle shapes. c) Kelvin probe measurements in trace and retrace (reverse) direction. Since the tip moves during compensation of the surface potential this leads to a shift of the two curves by 43 nm relative to each other.

References:

1) Nah, Y.-C.; Paramasivam, I.; Schmuki, P. Doped TiO_2 and TiO_2 Nanotubes: Synthesis and Applications, *ChemPhysChem* **2010**, *11*, 2698–2713.
2) Nicole, J.; Tsiplakides, D.; Pliangos, C.; Verykios, X. E.; Comninellis, C.; Vayenas, C. G. Electrochemical promotion and metal-support interactions. *J. Catal*. **2001**, 204, 23–34.
3) Lüth, H. *Solid surfaces, interfaces and thin films*, 4th ed., de Gruyter, Berlin, **2001**.
4) Yan, C.-H.; Yan, Z.-G.; Du, Y.-P.; Shen, J.; Zhang, C.; Feng, W. Controlled synthesis and properties of rare earth nanomaterials, in: Handbook on the Physics and Chemistry of Rare Earths, vol. 41, (Ed. Gschneidner, K. A.; Bünzli, J.-C. G.; Pecharsky V. K.), Elsevier, Amsterdam, **2011**, 275–472.
5) J. Kullgren, C. W. M. Castleton, C. Muller, D. M. Ramo, K. Hermansson, B3LYP calculations of cerium oxides, *J. Chem. Phys*. **2010**, *132*, 054110.
6) Scanlon, D. O.; Dunnill, C. W.; Buckeridge, J.; Shevlin, S. A.; Logsdail, A. J.; Woodley, S. M.; Catlow, C. R. A.; Powell, M. J.; Palgrave, R. G.; Parkin, I. P.; Watson, G. W.; Keal, T. W.; Sherwood, P.; Walsh, A.; Sokol, A. A. Band alignment of rutile and anatase TiO_2, *Nature Mat.***2013**, *12*, 798–801.
7) Choi, J.; Luo, Y.; Wehrspohn, R. B.; Hillebrand, R.; Schilling, J.; Gosele, U. Perfect two-dimensional porous alumina photonic crystals with duplex oxide layers, *J. Appl. Phys*. **2003**, *94*, 4757–4762.

8) Hay, P. J.; Martin, R. L.; Uddin, J.; Scuseria, G. E. Theoretical study of CeO_2 and Ce_2O_3 using a screened hybrid density functional, *J. Chem. Phys*. **2006**, *125*, 034712.

9) Pfau, A.; Schierbaum, K. D.; Göpel, W. The electronic structure of CeO_2 thin films - the influence of Rh surface dopants, *Surf. Sci*. **1995**, *331*, 1479–1485.

10) Asahi, R.; Taga, Y.; Mannstadt, W.; Freeman, A. J. Electronic and optical properties of anatase TiO_2, *Phys. Rev. B* **2000**, *61*, 7459–7465.

11) Henrich, V. E.; Cox, P. A. The surface science of metal oxides, Cambridge University Press, Cambridge, **1994**.

12) Perevalov, T. V.; Gritsenko, V. A.; Kaichev, V. V. Electronic structure of aluminum oxide: ab initio simulations of α and γ phases and comparison with experiment for amorphous films, *Eur. Phys. J. – Appl. Phys*. **2010**, *52*, 30501.

13) Electron work function of the elements, in: CRC Handbook of Chemistry and Physics, Section 12: Properties of Solids, (Ed. Haynes, W. M.), CRC Press, Boca Raton, Florida. 93th ed. **2012**, 114.